Dhofar 026, 457, 458, 459, 460, 461, 462, 463, 464, 465, 466, 467, 468

Anorthositic granulitic breccia

148, 99.5, 36.7, 31.5, 73.1, 33.7, 44.7, 24.3, 22.3, 70.7, 69.2, 36.2, 18.9 g

Figure 1: Photo of Dhofar 026 with a 1 cm cube for scale (photo from R. Korotev).

Introduction

Dhofar 026 (Fig. 1) was found in the Dhofar region of Oman (Figs. 2 and 3) in March, 2000 (Grossman et al., 2000). The 148 g brownish gray stone lacks fusion crust, but terrestrial weathering is not as significant as other desert meteorites. Smaller additional stones Dhofar 457-468 were found in April and July 2001 (Fig. 4), and are paired on the basis of their location of find, textures and chemical compositions.

Petrography and mineralogy

Dhofar 026 is a highly feldspathic, melt-rich breccia (Fig. 5), but there is some disagreement as to whether it is an impact melt breccia or an impact heated granulitic breccia (Warren et al., 2005; Cohen et al., 2004). Warren et al (2005) characterize the sample as comprised of roughly half aphanitic mono-mineralic plagioclase, and the other half a partially poikilitic "intergrowth" texture. Cohen et al. (2004) subdivide the "intergrowth" into pyroxene-plagioclase intergrowths (Fig. 6), and olivine-plagioclase

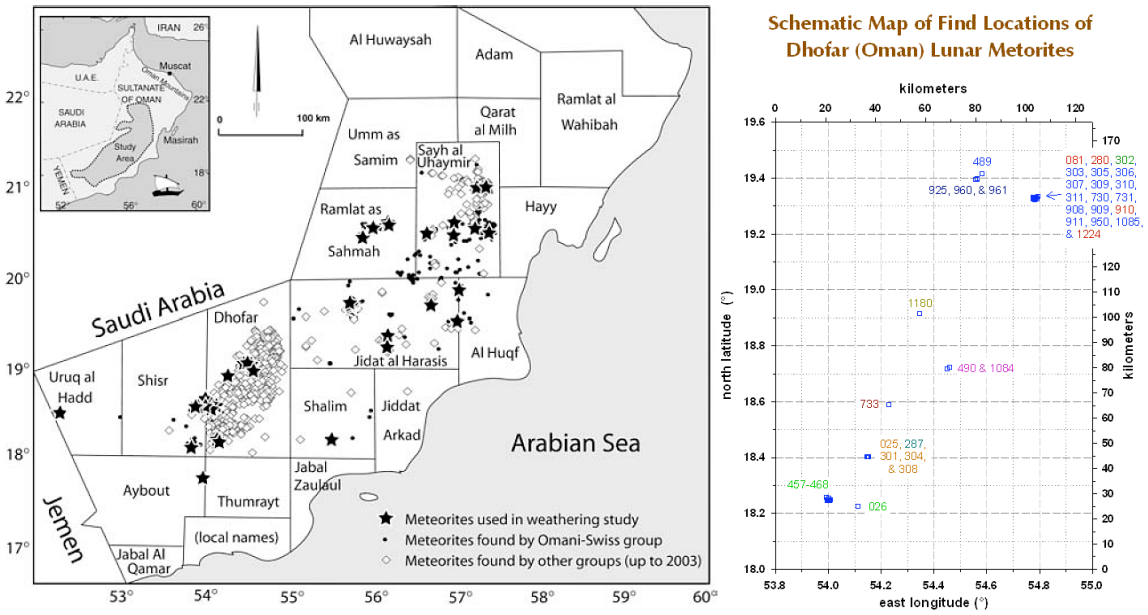

Figure 2: Map showing location of regions within Oman where meteorites have been recovered, such as Dhofar.

Figure 3: More detailed locations of the Dhofar meteorites, including Dho 026 and 457-468 (shown in green in lower left).

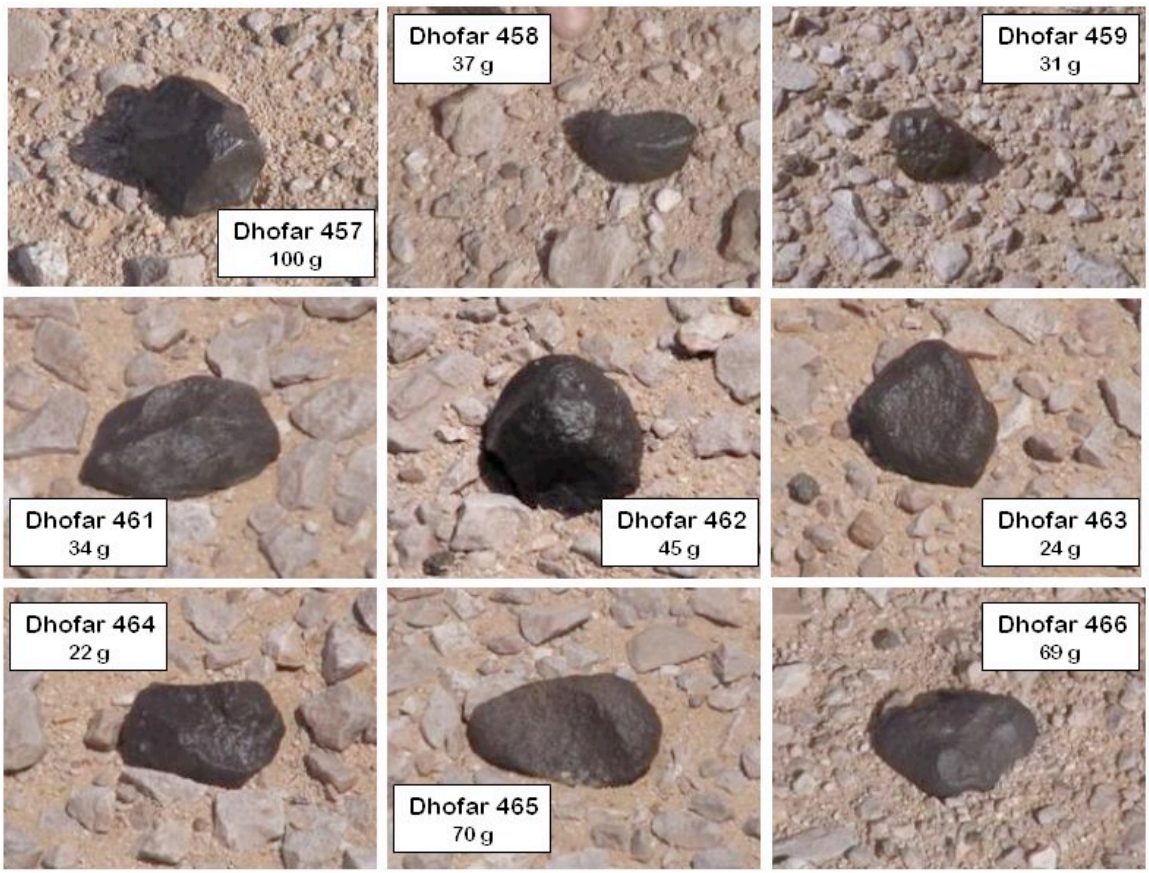

Figure 4: Selected images of additional smaller stones paired with Dho026 (photo from R. Korotev).

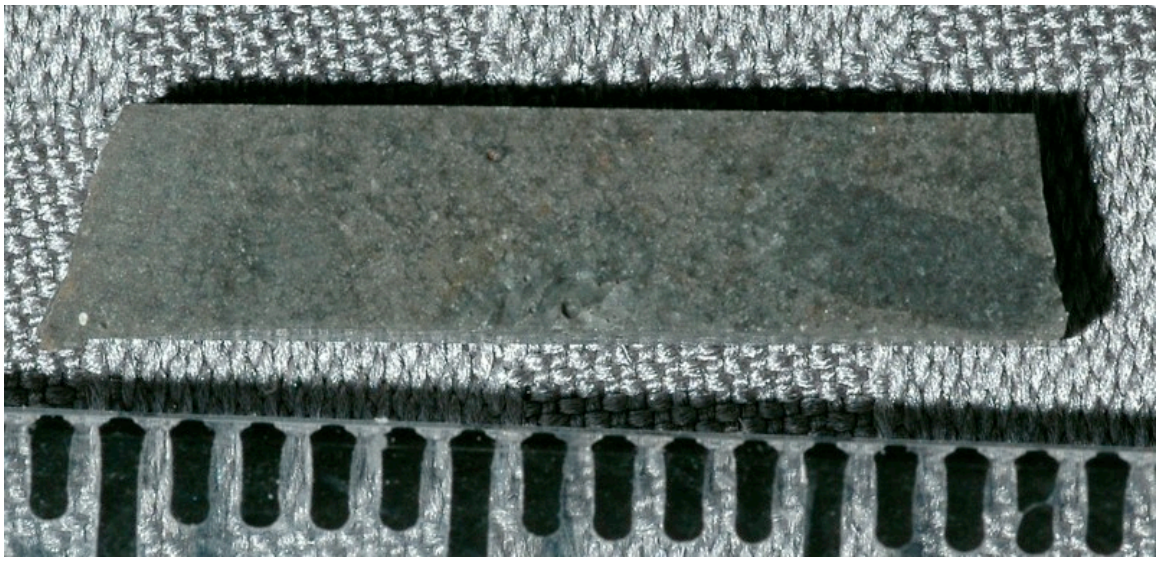

Figure 5: Photo of a slab of Dhofar 026, illustrating fine grained feldspathic nature. Scale bar at bottom is in mm. Photo from R. Korotev.

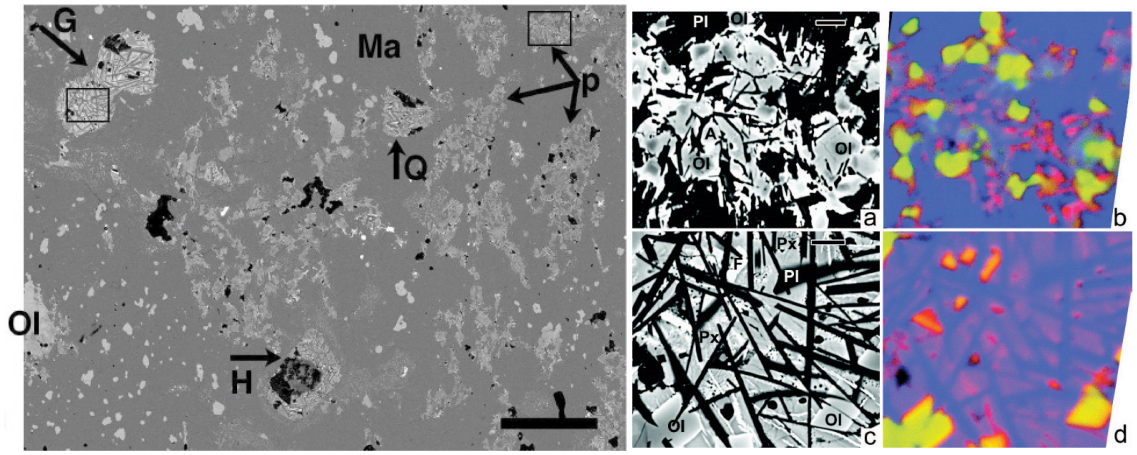

Figure 6: Back scattered electron image of a region of Dhofar 026 (left) illustrating the textures in this breccia, as well as highlighting several of the clast textures observed by Cohen et al. (2004) and Warren et al. (2005). Top right images (a and b) are from a pyroxene-plagioclase intergrowth (top right corner of left hand BSE image), and bottom right images (c and d) are from an ovoid globule (G in left hand image).

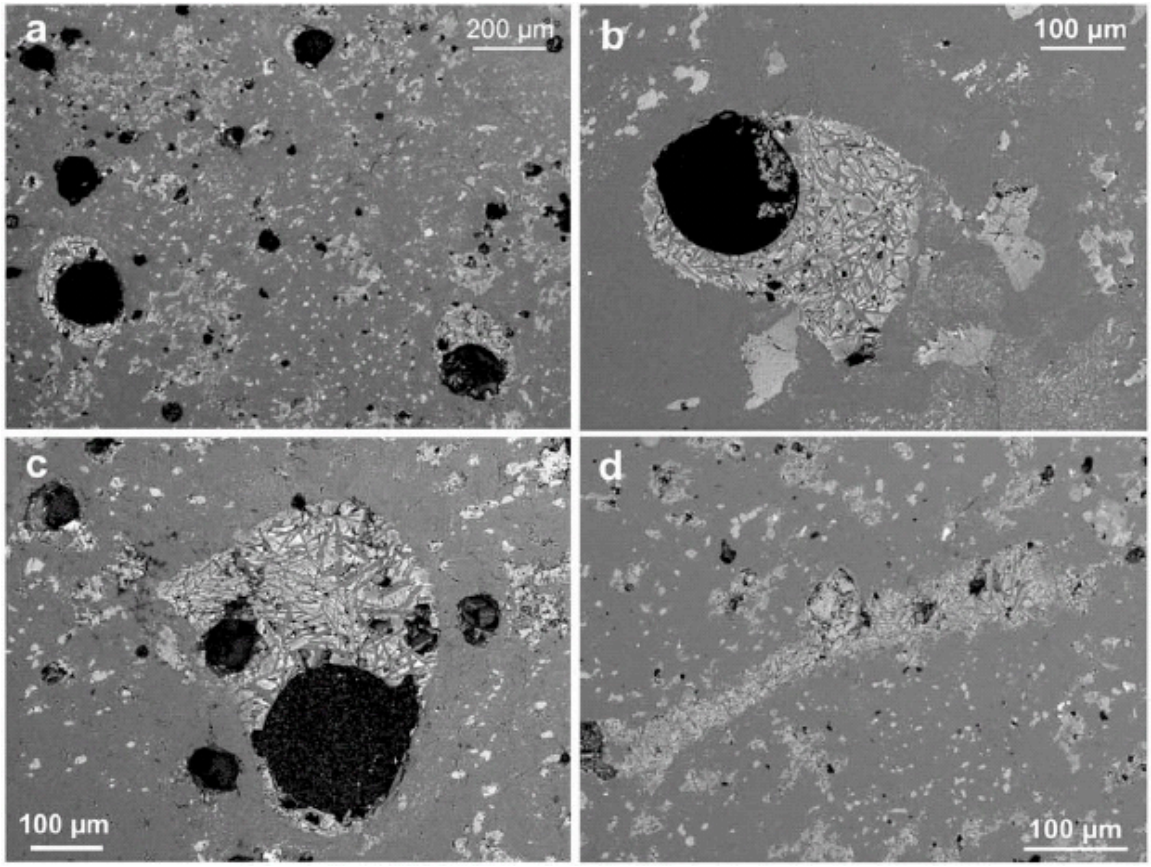

Figure 7: Four backscattered electron images of clasts from Dhofar 026 (and pairs), illustrating a) two typical spheroidal mafic impact melt globules (vesicular) from Dho 461, b) mafic impact melt globule from Dho 465, c) another mafic impact melt globule illustrating a nearly spherical vesicle, within Dho 461, and d) an elongated mafic impact globule from Dho 463 (from Warren et al., 2005).

intergrowths. They emphasize the common occurrence of granulitic textures in this breccia. Both studies highlight the unusual ovoid features that are present at less than 1% of the mode (Figs. 6 and 7). These globules are approximately 45% plagioclase, 35% pyroxene, and 20% olivine. The globules have a more mafic composition, and resemble the more mafic of the common impact melt breccias in the Apollo collection (Warren et al., 2005).

Plagioclase feldspar is largely anorthite-rich, from An_{96} to An_{98}, but the globules contain slightly more sodic feldspars (Fig. 8). Pyroxene compositions are similar to that expected for highlands materials (higher Mg#), but again the globules have a slightly different composition and are more FeO-rich (Fig. 9). On the other hand globule olivines have higher Mg# than the other lithologies in Dhofar 026 (Fig. 9).

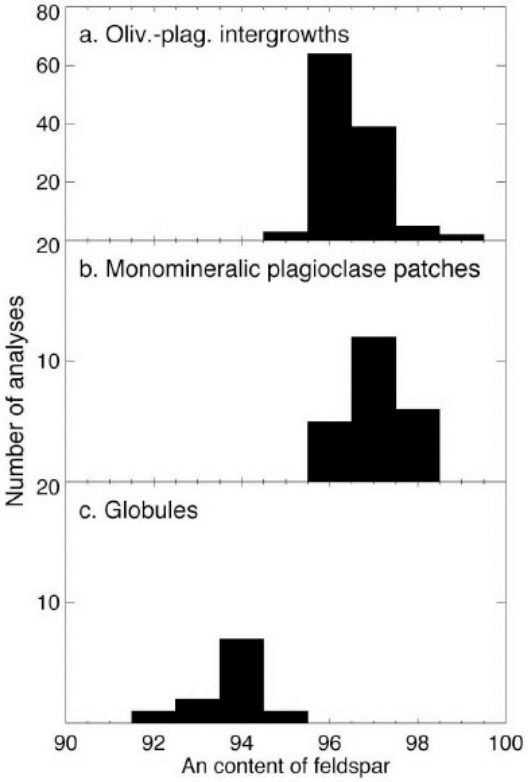

Figure 8: Feldspar compositions from intergrowths, globules and monomineralic areas in Dhofar 026 (from Cohen et al., 2004).

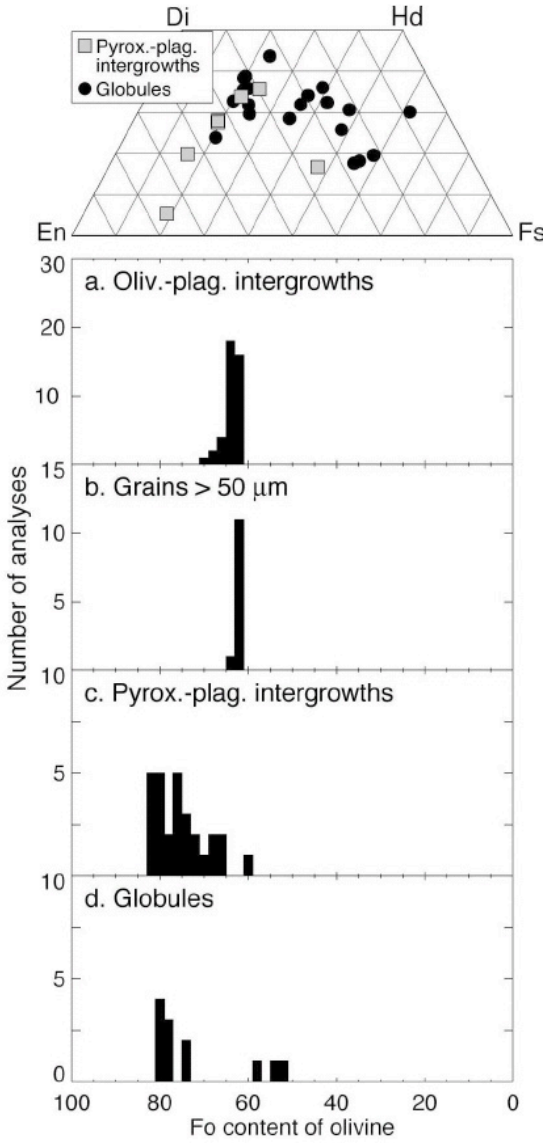

Figure 9: Pyroxene and olivine compositions from intergrowths and globules in Dhofar 026 (from Cohen et al., 2004).

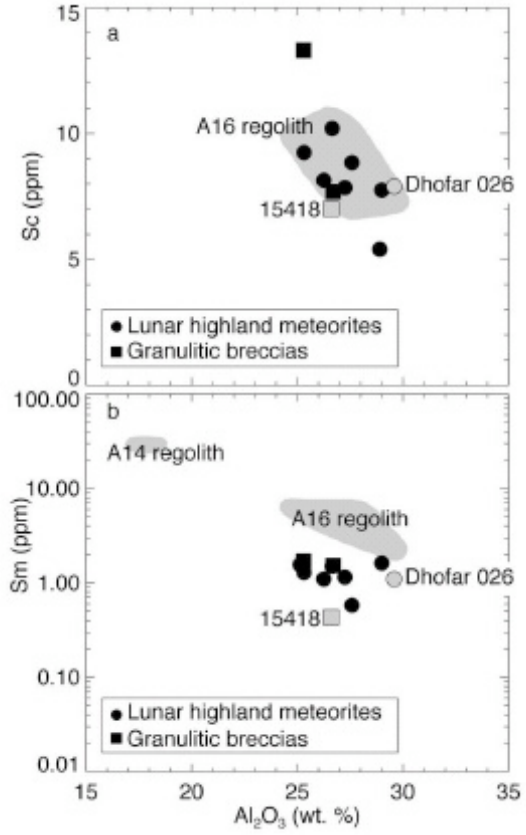

Figure 9: Sc and Sm (ppm) vs. Al_2O_3 for some lunar highlands meteorites including Dhofar 026 and also granulitic breccias (from Cohen et al., 2004).

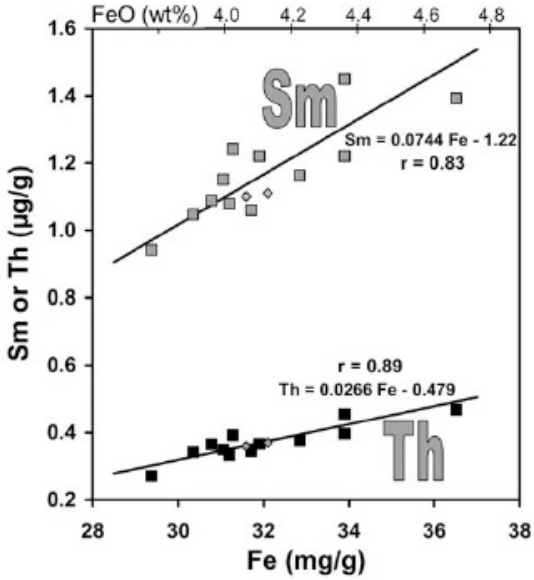

Figure 10: .Sc vs. Mg# and Ba vs. Sr for some of the Dhofar meteorites including Dhofar 025 (from Nazarov et al. (2004)

Chemistry

Dhofar 026 and its pairs have compositional features that make lunar feldspathic meteorites distinct from Apollo samples - they have high Al_2O_3 (~ 30 wt%; Fig. 9) and low FeO (3.8 to 4.7 wt%; Fig. 10). They have similar Sc contents compared to Apollo 15 and 16 breccias, but lower Sm, (Fig. 9; Warren et al., 2005; Cohen et al., 2004; Korotev et al., 2003). Rare earth elements (REE) are as high as QUE 93069 and Dhofar 025 - higher than many lunar feldspathic meteorites (Fig. 11). Enrichments of siderophile elements such as Ir seem anomalous (Warren et al., 2005) and may be due to contamination from sawing or otherwise.

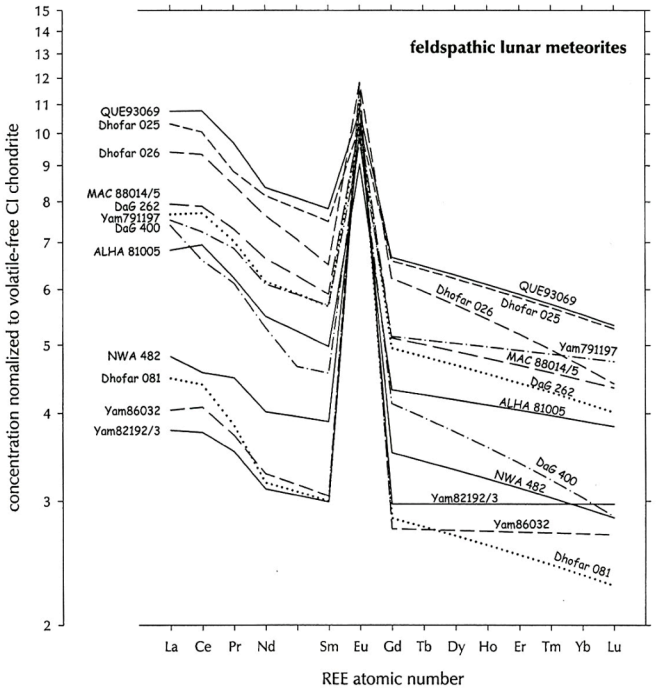

Figure 11: REE concentrations for Dho 026 compared to those for other lunar feldspathic meteorites (from Korotev et al., 2003).

Radiogenic age dating

Two kinds of chronologic studies have been completed on Dhofar 026. Cohen et al. (2002) have applied the laser fusion techniques to several individual clasts from Dho 026 and found an age clustering at 500 Ma, suggesting a young impact event. Fernandes et al. (2004) used the UV laser technique to date spots in Dhofar 026 and found a range of ages with those between 1.56 and 2.16 Ga possibly representing impact events. There is no other known chronologic data for these samples.

Cosmogenic isotopes and exposure ages

Several different studies have found Dhofar 026 to have very low noble gas and cosmogenic nuclide contents for lunar meteorites (Shkulyokov et al., 2001; Nishiizumi and Caffee, 2001; Fernandes et al., 2004). Regolith exposure times on the order of 10 Ma have been determined by all three studies. In addition, a short Earth-Moon transit time is suggested by ^{38}Ar, probably ~ 10 Ka (Fernandes et al., 2004; Nishiizumi et al., 2001), or perhaps even shorter based on ^{10}Be (4 Ka), ^{26}Al (2 Ka), and ^{36}Cl (3 Ka) (Nishiizumi et al., 2001).

Table 1: Chemical composition of Dho 026

		026	457	458	459	461	462	463	464	465	466	467	468	wm
reference	1	2	2	2	2	2	2	2	2	2	2	2	2	2
weight method	a,e,g	e	e	e	e	e	e	e	e	e	e	e	e	e
SiO_2 %	44.3	44.71	44.92	44.92	45.14	44.92	44.92	44.92	44.92	44.71	44.71	44.71	44.92	44.92
TiO_2	0.22	0.28	0.17	0.22	0.22	0.22	0.20	0.17	0.20	0.20	0.23	0.18	0.23	0.20
Al_2O_3	29.6	27.01	28.33	28.90	29.28	29.28	28.90	29.28	29.09	29.28	29.47	28.52	28.52	29.09
FeO	4.06	4.70	4.36	4.10	3.96	4.08	4.22	3.90	4.03	4.00	3.78	4.36	4.01	4.05
MnO	0.06	0.07	0.07	0.07	0.08	0.06	0.06	0.06	0.06	0.07	0.05	0.07	0.06	0.06
MgO	3.92	6.63	4.23	4.11	3.98	3.98	4.13	3.98	4.15	3.98	3.62	4.31	4.15	4.06
CaO	17	16.23	16.93	16.79	16.65	16.65	16.93	16.79	16.79	17.07	17.35	16.93	16.79	16.93
Na_2O	0.24	0.34	0.33	0.32	0.31	0.31	0.31	0.22	0.32	0.32	0.30	0.30	0.30	0.30
K_2O	0.08	0.05	0.04	0.04	0.04	0.04	0.03	0.03	0.03	0.04	0.03	0.04	0.04	0.04
P_2O_5	0.05													
S %														
sum														
Sc ppm	7.9	8.7	8.3	7.5	7.9	7.4	7.6	7.5	7.8	7.8	7.1	7.7	7.5	7.6
V		<20	16	18	15	15	20	20	18	23	18	22	18	19
Cr	547	630	620	560	610	550	570	570	590	590	520	580	550	570
Co	13.6	16.2	17.3	16	16.6	14.8	16.4	16	15.5	16	13.2	15.7	17	15.6
Ni	170	155	153	138	125	116	147	134	127	127	118	136	174	134
Cu														
Zn														
Ga		3.7	4.3	3.8	3.3	3.1	3.8	3.9	3.7	3.5	2.7	3.4	3.3	3.5
Ge														
As		<0.15	<0.26	0.18	0.1	<0.16	<0.36	0.17	<0.2	<0.21	<0.1	<0.34	0.15	
Se														
Rb														
Sr	200	128	209	254	540	350	206	890	630	670	310	300	1260	497

Y														
Zr	32	56	34	46	16	<50	39	33	33	33	30	36	49	35
Nb														
Mo														
Ru														
Rh														
Pd ppb														
Ag ppb														
Cd ppb														
In ppb														
Sn ppb														
Sb ppb		42	<150	48	40	21	34	24	<170	<40	36	<40	66	38
Te ppb														
Cs ppm	0.44	<0.05	0.126	0.071	0.085	0.082	0.081	0.082	0.074	0.085	0.058	0.069	<.120	0.078
Ba														
La	2.9	3.1	3.8	3.06	2.48	2.3	2.66	2.5	2.92	2.95	2.3	3.08	2.57	2.76
Ce	6.6	7.3	7.9	6.8	6.3	5.8	6.2	6.1	6.4	6.1	4.9	6.3	5.8	6.2
Pr														
Nd	3.8	5	5.3	4	3.2	3.6	3.6	3.6	4.1	4.1	3	4.1	3.8	3.8
Sm	1.1	1.39	1.45	1.22	1.09	1.06	1.16	1.05	1.24	1.15	0.94	1.22	1.08	1.14
Eu	1.1	0.78	0.86	0.79	0.78	0.71	0.79	0.69	0.76	0.78	0.75	0.73	0.73	0.76
Gd														
Tb	0.25	0.27	0.28	0.26	0.26	0.25	0.23	0.25	0.27	0.25	0.2	0.27	0.23	0.25
Dy		<1.34	1.94	1.76	1.53	1.8	1.54	1.08	1.59	1.41	1.4	1.8	1.53	1.55
Ho		0.35	0.43	0.37	0.29	0.29	0.35	0.26	0.41	0.31	0.3	0.32	0.28	0.33
Er														
Tm														
Yb	0.85	1.01	1.13	0.94	0.89	0.88	0.93	0.83	0.95	0.87	0.78	0.92	0.88	0.9
Lu	0.15	0.15	0.152	0.134	0.131	0.126	0.13	0.123	0.135	0.124	0.104	0.136	0.126	0.127
Hf	0.86	0.99	1.01	0.83	0.8	0.8	0.87	0.79	0.84	0.77	0.66	0.9	0.81	0.81
Ta	0.24	0.1	0.14	0.116	0.109	0.101	0.125	0.106	0.107	0.095	0.102	0.116	0.116	0.111
W ppb														
Re ppb														
Os ppb														
Ir ppb	6.3	487	13	5.2	5.6	5.3	6.3	6.1	5.5	5.2	4.6	6.5	7.1	15.5
Pt ppb														
Au ppb	9	4.1	7.8	11.4	17.8	16.1	23.7	10.4	19.8	17.6	6.3	5.3	13.4	12.5
Th ppm	0.36	0.47	0.45	0.37	0.37	0.34	0.38	0.34	0.39	0.35	0.27	0.4	0.33	0.36
U ppm		0.15	0.15	0.13	0.181	0.127	0.075	0.23	<0.13	<0.11	0.078	<0.13	0.092	0.13

technique (a) ICP-AES, (b) ICP-MS, (c) IDMS, (d) FB-EMPA, (e) INAA, (f) RNAA, (g) XRF

References: 1) Cohen et al. (2004); 2) Warren et al. (2005)

Table 1b. Light and/or volatile elements for Dho 026

		026	457	458	459	461	462	463	464	465	466	467	468	wm
reference	1	2	2	2	2	2	2	2	2	2	2	2	2	2
Li ppm														
Be														
C														
S														
F ppm														
Cl														
Br		1.7	1.9	1.9	1.6	1.34	2.8	1.2	1.36	1.8	1.13	1.9	2.1	1.6
I														
Pb ppm														
Hg ppb														
Tl														
Bi														

References: 1) Cohen et al. (2004); 2) Warren et al. (2005)
technique (a) ICP-AES, (b) ICP-MS, (c) IDMS, (d) FB-EMPA, (e) INAA, (f) RNAA, (g) XRF